Effect of crystallinity on the dielectric loss of sputter-deposited (Ba,Sr)TiO_3 thin films in the microwave range

Tae-Gon Kim, Jeongmin Oh, Taeho Moon, Yongjo Kim, and Byungwoo Park[a)]
School of Materials Science and Engineering, Seoul National University, Seoul 151-744, Korea

Young-Taek Lee and Sangwook Nam
School of Electrical Engineering and Computer Science, Seoul National University, Seoul 151-744, Korea

(Received 20 September 2002; accepted 16 December 2002)

The crystallinity dependence of the microwave dielectric losses in (Ba,Sr)TiO_3 thin films was investigated. The sputter-deposition temperatures were altered to vary the level of thin-film crystallinity on a Pt/Si substrate. The dielectric losses (tan δ) were measured up to 6 GHz without parasitic (stray) effects by using a circular-patch capacitor geometry and an equivalent-circuit model. The microwave dielectric losses increased from 0.0024 ± 0.0018 to 0.0102 ± 0.0017 with increasing crystallinity. These deteriorated dielectric losses showed a good correlation with the symmetry-breaking defects, as confirmed by Raman spectra at approximately 760 cm^{-1}, inducing microscopic polar regions above the Curie temperature of the bulk $(Ba_{0.43}Sr_{0.57})TiO_3$.

I. INTRODUCTION

(Ba,Sr)TiO_3 (BST) thin films have been studied intensively for use in microwave devices, such as phase shifters, band-pass filters, and frequency triplers.[1–3] This is due to its high-dielectric constant, relatively low loss, and high dielectric nonlinearity (tunability) in the microwave-frequency range.[1–6] In particular, dielectric loss is one of the most important factors for high-frequency applications when considering the efficiency of devices. Dielectric losses depend on the microstructures of the thin films, such as the phase, grain size, composition, strain, defects, etc.[1–9] Generally, pure paraelectric thin films, for example $ZrTiO_4$, show high quality factors ($Q = 1/\tan\delta$) in the crystalline phase, and Q is low in the amorphous phase.[9] However, there are reports showing that crystalline $(Ba_xSr_{1-x})TiO_3$ thin films (paraelectric phase with $0 \leqslant x \leqslant 0.6$ at room temperature[2]) have higher dielectric losses than the amorphous phase. In contrast, the dielectric constants and tunabilities show reverse behaviors (i.e., high in the crystalline phase and low in the amorphous phase).[7,10] Despite these reports, there have been few systematic studies on the correlations between the microstructures and the dielectric-loss behaviors of BST thin films.

Since dielectric losses have frequency-dependent behavior, it is necessary to investigate the dielectric losses in the GHz frequency range where the dielectric devices are operated. However, in spite of the microwave applications, many studies have been performed around the sub-MHz range.[1–3,5–7] In this paper, the correlations between the order of crystallinity and the dielectric losses of BST thin films were investigated systematically in the microwave-frequency range.

II. EXPERIMENTAL

Using radio frequency magnetron sputtering with a $(Ba_{0.5}Sr_{0.5})TiO_3$ target sintered at 1350 °C, BST thin films (approximately 250-nm thick) were deposited on 100-nm-thick Pt as a bottom electrode (stable up to 800 °C) with a $TiO_2/SiO_2/Si$ (100) substrate. The Ar (99.999%) to O_2 (99.995%) flow-rate ratio was 5 to 1, with an operating pressure of 1.3 Pa and an incident radio frequency power of 100 W. To acquire different levels of crystallinity, the deposition temperatures were varied from room temperature (RT) to 750 °C. X-ray diffraction (XRD) (M18XHF-SRA, MAC Science) with Cu K_α radiation was used to determine the degree of crystallinity of the thin films in the 2θ range of 20°–50°. (The diffraction peaks above 50° were insignificant due to their low intensities.) The Ba/Sr ratio was analyzed by electron probe microanalysis (JXA-8900R, JEOL). $BaTiO_3$ and $SrTiO_3$ crystals were used as standard samples for quantitative analysis of electron probe microanalysis.

a) Address all correspondence to this author.
e-mail: byungwoo@snu.ac.kr

 © 2003 Materials Research Society

The dielectric properties, such as the dielectric losses and dielectric constants, of the BST films in the GHz frequency range were measured with a circular-patch capacitor by a vector-network analyzer (HP 8510C). To remove the parasitic (stray) effects resulting from resistance in the bottom/top electrodes and contact with a Be–Cu coplanar waveguide (CPW) tip at the high-frequency range, an equivalent-circuit model with a parallel resistor/capacitor and a series resistor was applied. The reflection coefficient (Γ) of the device under test (DUT) was obtained by a one-port measurement technique and was converted to an impedance of the DUT. Details of the measurement technique are described in Refs. 9 and 11. The top electrode was an Au/Ag double layer, and Au was deposited on top of the Ag to make a reproducible contact with the CPW tip. Unpolarized Raman spectra (T64000, Jobin Yvon) were used in the right-angle scattering geometry with a 515-nm wavelength from Ar^+ laser at room temperature, to investigate the variation of the phonon modes in thin films.

III. RESULTS AND DISCUSSION

The Ba/Sr composition ratio was 0.43/0.57, which is similar to the value of the BST sputtering target. The composition was measured at several different points in the thin films and showed the same values with different deposition temperatures. From the XRD data shown in Fig. 1, a crystalline phase began to appear in the films deposited at 500 °C, and the XRD peaks [(100), (110), and (200)] became sharper overall as the deposition temperatures increased. The averaged full width at half maximum Δk [in scattering vector $k = (4\pi/\lambda)\sin\theta$] was estimated to be 0.86 ± 0.11 nm^{-1} at a deposition temperature of 500 °C and decreased to 0.43 ± 0.11 nm^{-1} at 600 °C, 0.42 ± 0.03 nm^{-1} at 700 °C, and 0.26 ± 0.01 nm^{-1} at 750 °C. (The overall widths are rather wider than some reported data, since thin films in this experiment have smaller grains or larger local strain.[1,3] This may be also caused by the excessive Ti atoms.[1]) This means that the overall crystallinity of the thin films was enhanced with the increase in the deposition temperatures. Raman spectroscopy also shows the enhancement of the structural perfection with the increase of deposition temperatures. The trend of crystallinity enhancement has been confirmed in many reports.[7–9] Some Au peaks were found from the residue of the top electrode.

Figure 2 shows the dielectric losses for the BST thin films as a function of the frequency with various deposition temperatures. The frequency dependence of the dielectric losses below 1 GHz and above 6 GHz and the overall noise were caused by the instrumental sensitivity and any uncompensated parasitic (stray) effects. Therefore, the dielectric losses between 1 and 6 GHz were averaged to visually express the dependence of the dielectric losses on the deposition temperatures, as shown in Fig. 3. The dielectric loss was 0.0024 ± 0.0018 at RT deposition and gradually increased to 0.0102 ± 0.0017 at 750 °C deposition. This means that the dielectric losses increased as the degree of crystallinity increased.

Raman spectroscopy was used to investigate the origin of the $(Ba_{0.43}Sr_{0.57})TiO_3$ dielectric-loss behavior, since it is sensitive to the changes in the crystallographic structure making appropriate phonon modes that affect the dielectric properties of the materials. Figure 4 shows the unpolarized Raman spectra of $(Ba_{0.43}Sr_{0.57})TiO_3$ thin films deposited at various temperatures. A broad peak centered at approximately 270 cm^{-1} [TO_3: A_1(TO)], a diffuse band at approximately 520 cm^{-1} [TO_4: A_1(TO), E(TO)], and a relatively weak peak near approximately 760 cm^{-1} [LO_4: A_1(LO), E(LO)] from the thin films were observed. (Dashed lines indicate the nonlinear

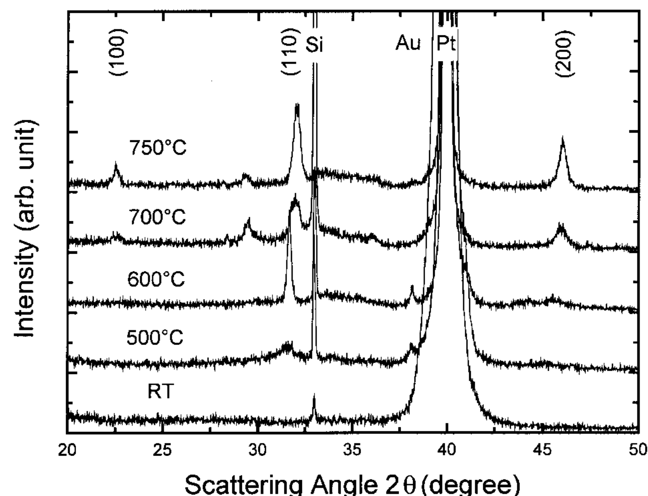

FIG. 1. XRD patterns of the $(Ba_{0.43}Sr_{0.57})TiO_3$ thin films deposited at temperatures ranging from RT to 750 °C.

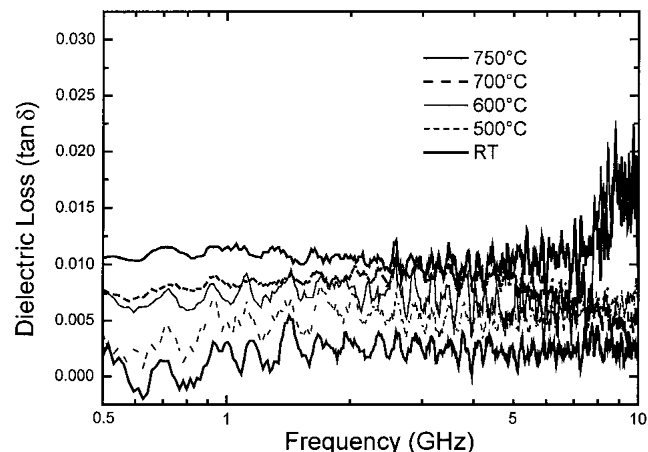

FIG. 2. Dielectric losses of the $(Ba_{0.43}Sr_{0.57})TiO_3$ thin films as a function of the frequency. From the bottom, the deposition temperatures increased from RT to 750 °C.

background by polynomial curve fitting.) Although these three modes are Raman inactive in cubic symmetry, the TO_3 and TO_4 modes were detected due to the local disorder of Ti ions along the ⟨111⟩ axes in the cubic phase.[12]

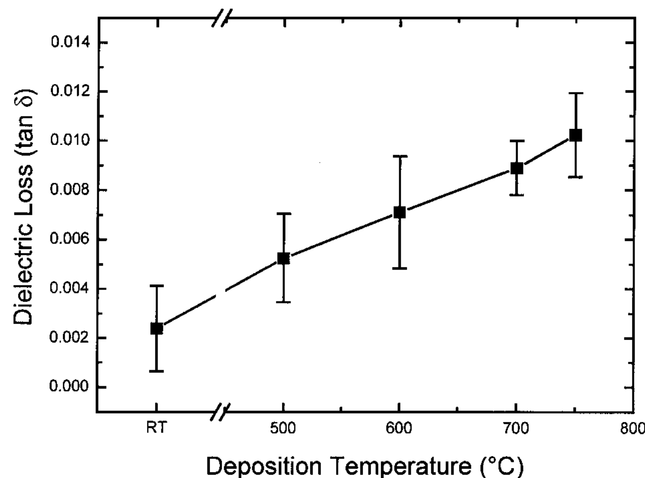

FIG. 3. Dielectric losses (averaged between 1 and 6 GHz) of the $(Ba_{0.43}Sr_{0.57})TiO_3$ thin films.

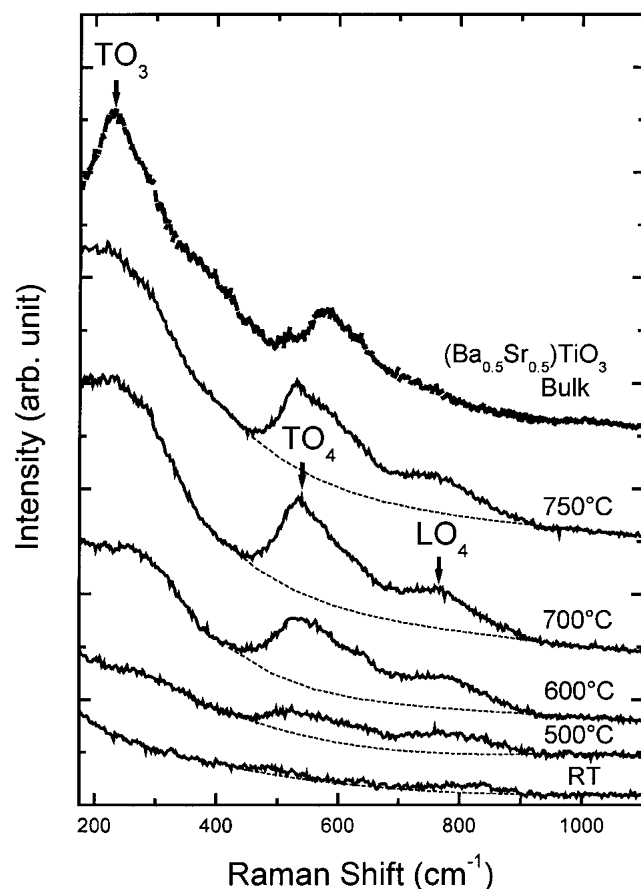

FIG. 4. Raman spectra of the $(Ba_{0.43}Sr_{0.57})TiO_3$ thin films deposited at various temperatures and compared with the bulk $(Ba_{0.5}Sr_{0.5})TiO_3$.

In addition, TO_4 and LO_4 result from the shift of Ti ions along the *c* axis or the formation of zigzag distortion of Ti–O–Ti bonds.[12–14] Accordingly, only the LO_4 phonon mode can reflect the remnant polarization.[13–15] The thick dotted curve in Fig. 4 is the Raman spectrum of bulk $(Ba_{0.5}Sr_{0.5})TiO_3$ (the sputtering target) as reference data.

The broad band at approximately 520 cm^{-1} includes the weak modes near 560 and 620 cm^{-1}, in addition to the TO_4 [A_1(TO), E(TO)]. These extra modes originated from the departure of the Ti ions from the regular sites in the BST lattice. The mode at approximately 560 cm^{-1} is due to the disordered paraelectric phase, and the approximately 620-cm^{-1} peak is attributed to the intergrain stresses that change the Ti–O bonds.[12,16,17]

To obtain notable trends in the LO_4 (approximately 760 cm^{-1}) and TO_4 (approximately 520 cm^{-1}) modes as a function of the deposition temperature or crystallinity, the Raman spectra were fitted with four Lorentzian functions. Figure 5 shows the Raman spectra of the thin films deposited at 700 °C after background removal. Different line shapes with more fitting parameters, such as Breit–Wigner–Fano function considering the asymmetric property of the peaks,[18,19] did not alter the overall fitted intensity notably. The integrated intensity of the TO_4 mode at approximately 520 cm^{-1} grows overall as the deposition temperature increases, as shown in Fig. 6. This phenomenon can be interpreted as an enhancement of the order of the basic structural perfection making the appropriate phonon modes. In addition, the growth of the integrated intensity of the LO_4 mode at approximately

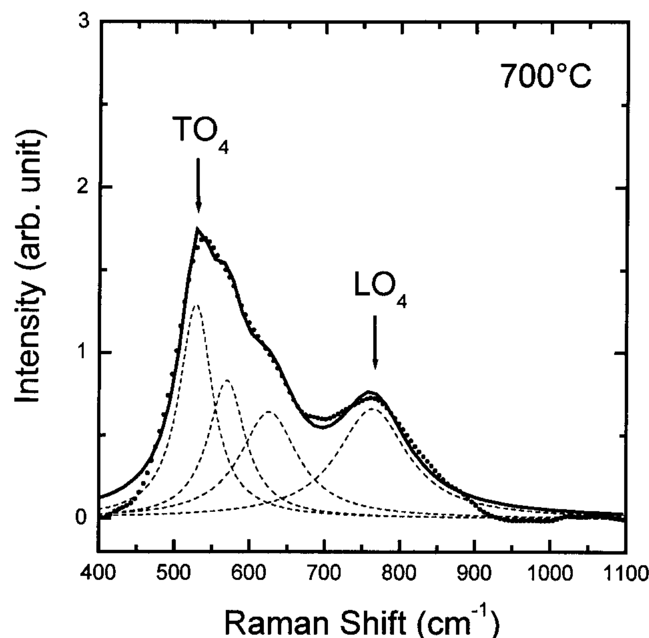

FIG. 5. Raman spectra of the thin film deposited at 700 °C, after background removal. Four peaks at ~520 (TO_4 mode), ~560, ~620, and ~760 cm^{-1} (LO_4 mode) were fitted by Lorentzian functions.

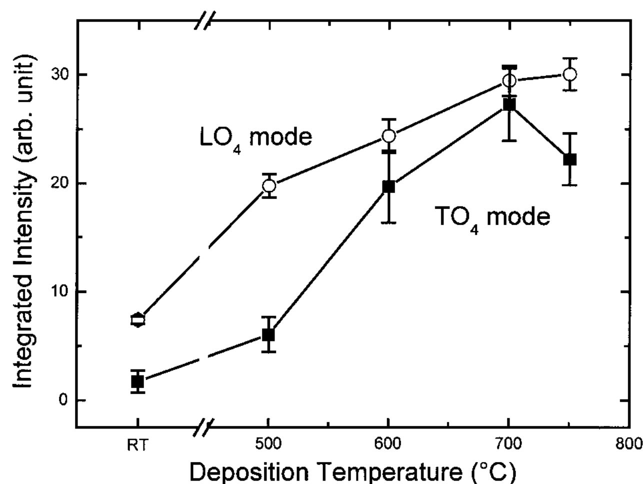

FIG. 6. Integrated Raman-peak intensities from thin films deposited at various temperatures. The LO_4 mode intensity at ~760 cm^{-1} is a characteristic feature of remnant polarization, and the TO_4 (~520 cm^{-1}) and LO_4 modes represent the order of structural perfection.

760 cm^{-1} means that the amount of remnant polarization is increased.[13,14] Two peaks near 560 and 620 cm^{-1} also show behavior similar to that of Fig. 6.

The *P–V* hysteresis curves were acquired under a virtual ground mode at 1 kHz to investigate the properties of the remnant polarization detected from the LO_4-mode peak. However, any vivid remnant polarization could not be observed in all the thin films. Since the remnant polarization measured by the hysteresis curves originates from the global long-range ferroelectric ordering,[13,20] it can be considered that the local short-range effects cause the remnant polarization detected by Raman spectroscopy. The defect-induced local remnant polarization, introduced in many studies,[13,14,18,20] was suggested as a reliable candidate of the local short-range effects. Due to a certain degree of orientational disorder, the *P–V* hysteresis curves can hardly detect them.[13] The local short-range effects that induce the remnant polarization may result from various defects, such as vacancies and substitutional/interstitial solutes. In particular, oxygen vacancies are known to be the most common defects in titanate thin films for local remnant polarization.[18,21] The main point is that dilute symmetry-breaking defects cause microscopic polar regions above the Curie temperature. A local dipole moment induced by symmetry-breaking defects polarizes the adjacent defect-free (perfect) unit cells within a neighborhood whose size depends on the dielectric constant of the host lattice.[13,14,22] Therefore, it is proposed that the increase in the LO_4-mode intensity originates from the growth of microscopic polar regions in the BST thin films.

The growth of polar regions can be indirectly confirmed by an improvement in the dielectric constants, since the sizes of the microscopic polar regions grow with the increasing dielectric constants.[13,14] Figure 7 shows that the dielectric constants increase from 10.29 ± 0.02 at RT to 243 ± 1 at 750 °C deposition. The relatively low dielectric constants in comparison to the reported data may originate from the excessive Ti atoms.[1] Despite the many defects in the thin films with a lower level of crystallinity, there is less remnant polarization, because the symmetry-breaking defects cannot polarize the adjacent unit cells well, owing to the very low-dielectric constant (polarizability) of the host lattice. It is clear that thin films with poor crystallinity have low-dielectric constants.[7,8] Moreover, not all defects in thin films with lower crystallinity are symmetry-breaking defects. There are many non-symmetry-breaking defects, which will not couple linearly with the remnant polarization and just cause a static atomic displacement.[15,22] In the bulk samples, the LO_4-mode Raman peak was not detected, as shown in Fig. 4, despite the high-dielectric constants. The difference between bulk and thin films may come from the intrinsic and extrinsic strains, which enhance the occurrence of local polar region, evolved during the thin-film deposition.[23,24]

For paraelectric BST thin films, the existence of local ferroelectric regions has been observed with confocal scanning optical microscopy and apertureless near-field scanning optical microscopy by Hubert *et al.*[23,25] They reported that the sizes of the ferroelectric nanodomains are <5 nm,[25] which are similar to the sizes of the defect-induced microscopic polar region (approximately 1 nm).[15]

Tagantsev showed theoretically that noncentrosymmetric crystals have much higher dielectric losses than centrosymmetric crystals,[26] and Vendik *et al.* reported that the electrostriction effects introduce high dielectric losses in the microwave-frequency range.[27] Consequently, the increase in the dielectric losses with the

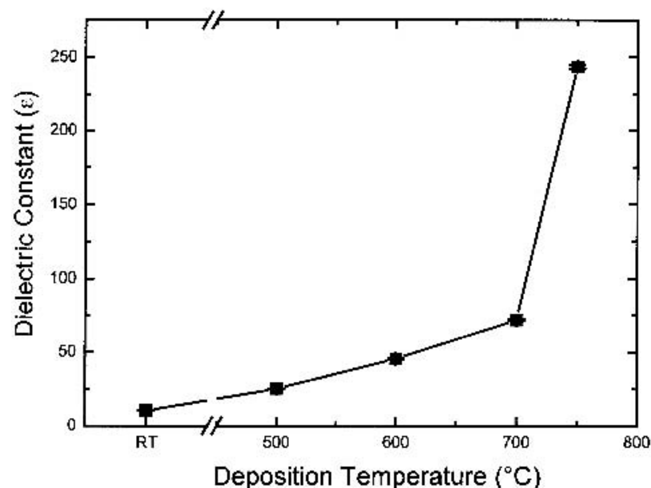

FIG. 7. Dielectric constants (averaged between 1 and 6 GHz) of the $(Ba_{0.43}Sr_{0.57})TiO_3$ thin films deposited at various temperatures.

enhancement of crystallinity may originate from the growth in the microscopic polar regions, which cause high dielectric losses.

IV. CONCLUSIONS

In summary, the correlation between the level of crystallinity and the dielectric losses of BST thin films was investigated. A circular-patch capacitor and an equivalent-circuit model effectively measured the dielectric properties in the microwave-frequency range (1–6 GHz). As the deposition temperatures increased, the degree of crystallinity increased, and the dielectric losses also increased. From Raman-spectra analysis (especially the LO_4 mode), it is proposed that the higher dielectric losses in good crystalline BST thin films originate from the occurrence of microscopic polar regions. The deterioration in the quality factors with increasing crystallinity was correlated with the enhanced dielectric constants.

ACKNOWLEDGMENTS

The authors wish to acknowledge the contributions of Min Kyung Choi, Hee Kyung Kang, and Prof. In-Sang Yang for materials characterization and their useful advice. This work was supported by the Korea Research Foundation (Grant KRF-2002-041-D00303).

REFERENCES

1. J. Im, O. Auciello, P.K. Baumann, S.K. Streiffer, D.Y. Kaufman, and A.R. Krauss, Appl. Phys. Lett. **76,** 625 (2000).
2. Y. Gim, T. Hudson, Y. Fan, C. Kwon, A.T. Findikoglu, B.J. Gibbons, B.H. Park, and Q.X. Jia, Appl. Phys. Lett. **77,** 1200 (2000).
3. P. Padmini, T.R. Taylor, M.J. Lefevre, A.S. Nagra, R.A. York, and J.S. Speck, Appl. Phys. Lett. **75,** 3186 (1999).
4. W. Chang, C.M. Gilmore, W-J. Kim, J.M. Pond, S.W. Kirchoefer, S.B. Qadri, D.B. Chirsey, and J.S. Horwitz, J. Appl. Phys. **87,** 3044 (2000).
5. S.K. Streiffer, C. Basceri, C.B. Parker, S.E. Lash, and A.I. Kingon, J. Appl. Phys. **86,** 4565 (1999).
6. B.H. Park, E.J. Peterson, Q.X. Jia, J. Lee, X. Zheng, W. Si, and X.X. Xi, Appl. Phys. Lett. **78,** 533 (2001).
7. B.H. Park, Y. Gim, Y. Fan, Q.X. Jia, and P. Lu, Appl. Phys. Lett. **77,** 2587 (2000).
8. I.N. Zakharchenko, M.G. Radchenko, L.A. Sapozhnikov, E.V. Sviridov, and V.P. Dudkevich, Crystallogr. Rep. **43,** 131 (1998).
9. Y. Kim, J. Oh, T-G. Kim, and B. Park, Appl. Phys. Lett. **78,** 2363 (2001); T. Kim, J. Oh, B. Park, and K.S. Hong, Appl. Phys. Lett. **76,** 3043 (2000).
10. W. Chang, J.S. Horwitz, W-J. Kim, C.M. Gilmore, J.M. Pond, S.W. Kirchoefer, and D.B. Chrisey, in *Materials Issues for Tunable RF and Microwave Devices*, edited by Q. Jia, F.A. Miranda, D.E. Oates, and X. Xi (Mater. Res. Soc. Symp. Proc. **603,** Warrendale, PA, 2000), p. 181.
11. Z. Ma, A.J. Becker, P. Polakos, H. Huggins, J. Pastalan, H. Wu, K. Watts, Y.H. Wong, and P. Mankiewich, IEEE Trans. Electron Devices **45,** 1811 (1998).
12. Y.I. Yuzyuk, V.A. Alyoshin, I.N. Zakharchenko, E.V. Sviridov, A. Almeida, and M.R. Chaves, Phys. Rev. B **65,** 134107-1 (2002).
13. J. Toulouse, P. DiAntonio, B.E. Vugmeister, X.M. Wang, and L.A. Knauss, Phys. Rev. Lett. **68,** 232 (1992).
14. H. Uwe, K.B. Lyons, H.L. Carter, and P.A. Fleury, Phys. Rev. B **33,** 6436 (1986).
15. C. Raptis, Phys. Rev. B **38,** 10007 (1988).
16. R. Naik, J.J. Nazarko, C.S. Flattery, U.D. Venkateswaran, V.M. Naik, M.S. Mohammed, G.W. Auner, J.V. Mantese, N.W. Schubring, A.L. Micheli, and A.B. Catalan, Phys. Rev. B **61,** 11367 (2000).
17. S-Y. Kuo, W-Y. Liao, and W-F. Hsieh, Phys. Rev. B **64,** 224103-1 (2001).
18. A.A. Sirenko, I.A. Akimov, J.R. Fox, A.M. Clark, H-C. Li, W. Si, and X.X. Xi, Phys. Rev. Lett. **82,** 4500 (1999).
19. D.G. McCulloch and S. Prawer, J. Appl. Phys. **78,** 3040 (1995).
20. U. Bianchi, W. Kleemann, and J.G. Bednorz, J. Phys.: Condens. Mater **6,** 1229 (1994).
21. R. Waser and D.M. Smyth, in *Ferroelectric Thin Films: Synthesis and Basic Properties*, edited by C. P. de Araujo, J.F. Scott, and G.W. Taylor (Gorden and Breach, Amsterdam, The Netherlands, 1996), p. 47.
22. B.I. Halperin and C.M. Varma, Phys. Rev. B **14,** 4030 (1976).
23. C. Hubert, J. Levy, A.C. Carter, W. Chang, S.W. Kiechoefer, J.S. Horwitz, and D.B. Chrisey, Appl. Phys. Lett. **71,** 3353 (1997).
24. D.A. Tenne, A.M. Clark, A.R. James, K. Chen, and X.X. Xi, Appl. Phys. Lett. **79,** 3836 (2001).
25. C. Hubert and J. Levy, Appl. Phys. Lett. **73,** 3229 (1998).
26. A.K. Tagantsev, Appl. Phys. Lett. **76,** 1182 (2000).
27. O.G. Vendik and L.M. Platonova, Sov. Phys. Solid State **13,** 1353 (1971).